AIMS Geosciences

AIMS Geosciences, 11(2): 442–467.
DOI: 10.3934/geosci.2025018
Received: 03 February 2025
Revised: 23 April 2025
Accepted: 27 April 2025
Published: 20 May 2025

https://www.aimspress.com/journal/geosciences

Communication

Geotechnical characterization of residual granite soils. The test site of Polytechnic Institute of Guarda (Portugal)

Carlos Rodrigues[1,*], Nuno Cruz[2] and Manuel Cruz[3]

[1] Department of Civil Engineering, Polytechnic Institute of Guarda, Portugal, Avenida Dr. Francisco Sá Carneiro, 50, 6300-559 Guarda, Portugal
[2] Mota-Engil Global, Geology and Geotechnics Dept, Rua Rêgo Lameiro, 38, 4300-454 Porto, Portugal
[3] Mathematical Eng. Lab, Polytechnic Institute of Porto, R. António Bernardino de Almeida, 431 Porto, 4200-072 Porto, Portugal

* **Correspondence:** Email: crod@ipg.pt; Tel: +351271220100.

Abstract: The geotechnical characterization of residual soils is a complex matter and is not always successful because current interpretation methodologies dedicated to sedimentary soils do not adequately respond to the behavior of this type of soils. The problem has been under scope by several Portuguese and international institutions. The work carried out in the experimental Site of the Polytechnic Institute of Guarda (IPG) since 2003, constituted by residual soils and decomposed rocks of the local granite massif, is highlighted herein. The work was strongly supported by MOTA-ENGIL (Portuguese construction company) and the Laboratory of Math Engineering (LEMA, Polytechnic Institute of Porto). The characterization of the test site and the respective research work is presented. The research work involved interpretation of in situ tests (SDMT, SCPTu, PMT, SPT, DPSH, and geophysical tests), tests in controlled chambers (DMT, geophysical, and suction tests), and laboratory tests (oedometric tests, direct shear tests, and triaxial tests with several stress paths). The tests were performed on natural structured soils, artificially cemented mixtures, and unstructured soils. Advanced math and statistical analysis were applied in the development of new correlations to obtain geotechnical parameters representative of these soils. Furthermore, the work also allowed to recognize the physical characteristics of the materials and better understand their mechanical behavior.

Keywords: in situ testing; experimental site; structured soils; granitic residual soils

1. Introduction

The north, center, and interior south of Portugal is greatly represented by granitic formations in several weathering stages, from unweathered massif to the corresponding residual soils. The adequate characterization of these formations is of great importance to support design and construction works. The decomposed to highly weathered materials resulting from the physical and chemical weathering of original massifs are commonly designated as intermediate geo-materials (IGM), while the consequent residual soils are saprolites, both quite different from sedimentary deposits where classical soil mechanics is applied. The main differences are related to the presence of cemented structures in residual masses, inherited from the original massif, which are not present in common sedimentary deposits, as well as to the absence of the overconsolidation processes that are usual in sedimentary soils. Therefore, direct application of classical soil mechanics in the interpretation of the mechanical behavior of these residual masses frequently leads to misinterpretations, particularly when using in situ testing that is strongly based on sedimentary approaches for their interpretation and parametrization.

In terms of shear strength, the granitic residual masses under study exhibit a cohesive-frictional drained behavior, while the common in situ interpretation methodologies only obtain angles of shearing resistance in granular soils and undrained strength in cohesive soils. As a consequence, cohesion intercept is not achievable by common interpretation methodologies, while the angle of shearing resistance is overestimated because the cohesive contribution is interpreted as friction contribution [1]. In turn, stress-strain behavior is characterized by the presence of two yield points; the first (1^{st} yield) is related to the beginning of breakage of cementation structure, and the second (2^{nd} yield or generalized yield) is related to the complete destruction of cemented structure, which is not present in usual sedimentary soils. Experimental work has also shown the deviation of the hyperbolic model, commonly used in sedimentary soils to obtain modulus degradation curves [2,3].

According to this, a proper geotechnical characterization is deeply dependent on triaxial testing, which is insufficient to cover the usual heterogeneity of residual masses (too many tests would have to be performed). Furthermore, triaxial tests depend on the quality of sampling, but the level of disturbance in residual masses can be quite damaging. In fact, the disturbance in these materials is mainly related to the penetration and extrusion phases that affect the stability of the cementation structure. The principal consequences are the partial loss of strength (cohesive intercept results lower than reality), while the stress-strain data usually misses the first yield. Therefore, the use of in situ tests to characterize these masses is unavoidable, but new methodologies of interpretation are required. For these purposes, only multi-parametric tests can be expected to derive simultaneously cohesive intercept and angles of shear resistance. Moreover, the combination of in situ mechanical and geophysical tests can also be very useful to derive the deformability modulus and respective degradation curves.

The IPG experimental site was created in 2003 and comprises an important laboratorial structure that include the usual tests (triaxial with internal instrumentation, shear box, oedometric) and a large-scale calibration device (controlled-condition chamber, CCC) where it is possible to remold samples with proper dimensions to offer the possibility of controlled in situ test executions ($1 \times 1 \times 1.5$ m). The site was created with the intention of developing adequate practices for understanding and characterizing the mechanical behavior of local residual masses, to support efficient design when dealing with these materials. The main goals of the program can be summarized as follows:

a) Launch bridges between Guarda and Porto granitic formations, since the latter constitutes the main source of information on Portuguese granites, both by the work developed by FEUP [1,5,6] and the regional Porto geotechnical map [7] that incorporates rich and varied geotechnical testing data of these (and other) materials.
b) Understand the differences between the mechanical behavior of natural granite residual soils and the behavior of these same soils when excavated and compacted (remolded).
c) Understand the differences between the mechanical behavior of natural and artificially cemented mixtures, since the latter are unavoidable in settling experimental frames related to cementation structures.
d) Establish methodologies to detect cemented structures (SBT diagrams) and properly derive geotechnical parameters departing from multi-parametric in situ tests, such as (S)DMT, (S)CPTu, and PMT, adequately controlled by laboratory tests.

The main achievements within the global framework are presented and discussed herein.

2. Porto and Guarda geologic background

Porto and Guarda cities are located in two similar Hercynian granitic environments that are 125 km apart from each other (Figure 1).

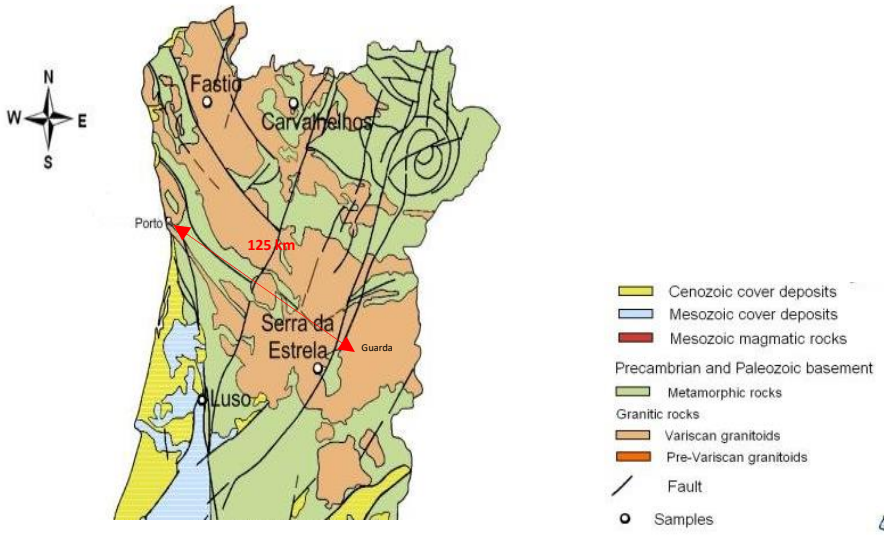

Figure 1. Simplified geological map of North and Center Portugal (adapted from the geological map of Portugal).

Both Porto and Guarda are integrated within the same climate zone, defined as warm summer, temperate, Mediterranean climate (Csb) according to Koppen climate classification [4], which favors the weathering of the granitic rock mass, turning the granite masses into permeable sandy frames.

From a geological point of view, Guarda granitic formation is within the geological complex responsible for the formation of Estrela massif, the highest mountain on the Portuguese mainland. The geologic history of the massif started in the Precambrian (650 million years) with marine deposition

that kept going on through the Cambrian (500 million years), followed by diagenesis and metamorphism responsible for the formation of schist and greywacke sequences, quite common in the Portuguese mainland. Afterward, three phases of Hercynian orogeny (305 million years) took place, during which the main granitic mass was developed, followed by its erosion and uplift. The Guarda granitic formation is represented by a leucomesocratic granite with quartz, sodic and potassium feldspars, biotite and muscovite, as well as kaolin, sericite, and chlorite as products of chemical weathering [1,5]. The variation of water level ranges from a submerged stage in the wet season, followed by drying up in depth during the summer, creating conditions for continuous weathering.

In turn, the granites represented in the Porto area (Porto granitic formation) are installed in a Hercynian NW–SE platform that is laterally confined by two metamorphic complexes: Schist–Greywacke complex at Northeast and Foz-do-Douro metamorphic complex at Southwest. The latter is connected with the Porto–Tomar fault, one of the main geotectonic contacts of the Iberian Peninsula that divides the Central–Iberian Zone from the Ossa-Morena Zone of the old Hesperic massif. The studied area is located on the border of the former. In general, it can be said that actual topography is the result of a long surface modeling, starting at the end of the Hercynian orogeny (270 million years ago). Porto granites are approximately 300 million years old and were installed at around 10 km depth. Due to the joint and fault systems generated by Hercynian or later movements, the granitic mass has risen way up to the surface, where it mostly rests today. The Porto granitic formation can be described as a leucocratic alkaline rock, comprising a mixture of glassy quartz, white alkali-feldspar often in mega-crystals, biotite, and muscovite, with the latter prevailing in sodic and potassic feldspars. Kaolin, sericite, and chlorite constitute the mineralogy of the chemical weathering products. The alkali feldspar usually presents higher grain size and is mostly orthoclase, but sometimes microcline. As for plagioclases, oligoclase-albite and albite are commonly present [5,7,8]. Other variations of the main formation are present, showing small differences and having a minor representation, such as the Granite of Contumil (mega-crystals of feldspars), Granite of Póvoa de Varzim (sometimes with a gneissic texture), and the Granite of Campanhã, all showing gradual transitions to the main body.

The weathering evolution of both granitic formations is very similar and consists mainly of the hydrolysis of feldspars into kaolin clay and some oxidation of biotite and iron-magnesium minerals. As the weathering progresses, the original bonds between the grains break, and feldspars and micas become unstable, generating a network of intragranular voids. As a consequence, quartz (stable) grains are bonded by weathered (unstable) grains of feldspars and micas to form a solid skeleton with variable porosity, according to the attained weathering level.

From an identification point of view, Porto and Guarda residual masses are characterized by a well graded silty sand to sandy silt with low plasticity (mostly non-plastic), classified as SM or SM-SC and A(a) and A(b), according to the Unified Classification [9] and Wesley Residual Soil Classification [10], respectively. The petrographic index, χ_d [11], which relates percentages of weathered and unweathered grains, falls within 0.27 and 0.64 in both residual masses, reflecting the high weathering degrees that can be found in the local massifs [6].

The geotechnical evolution through weathering of both granitic formations leads to similar geotechnical units in Porto and Guarda, falling within the same geotechnical ranges, namely in terms of grain size distributions, plasticity indexes, permeability, uniaxial strength, cohesive intercepts, angles of shear resistance, and deformability moduli. In fact, these granitic saprolites (residual soils) fall within two basic units generally characterized by N_{SPT} ranges of 10–30 blows (G1) and 30–60

blows (G2), while the IGMs decomposed, W_5 (G3), and highly weathered, W_4 (G4) massifs are represented by values higher than 60 blows, respectively with penetrations within 15–30 cm and lower than 15 cm [1]. The in situ void ratios generally fall within 0.4–0.8, generating angles of shearing resistance of 32º to 40º. Coefficients of permeability usually range between 10^{-6} and 10^{-7} m/s, with no important variations through these weathering stages, globally reflecting the very similar grain sizes and plasticity, despite their weathering stage. Thus, drained behavior is expected and observed in the most common load situations. Table 1 summarizes the typical in situ and laboratory parameter ranges related to these granitic materials. These ranges were obtained using the data available in the Porto Geotechnical map, calibrated by the results obtained in the research programs performed in Porto and Guarda. CPTu and DMT results are not present in the Porto Geotechnical map; thus, the presented ranges were obtained during the global research presented herein.

Table 1. In situ typical ranges of Portuguese granites.

Test	Test parameter	G1	G2	G3
Classification	Unified classification	SC, SM	SM	SM
Classification	Wesley classification	A(a)	A(b)	A(b)
Identification	#200 sieve passing %	<35	<25	<25
Identification	Plasticity index	<10	NP	NP
Lab/DMT	Unit weight, γ (kN/m^3)	17–19	18–20	20–22
Lefranc tests	Coef. permeability, k (m/s)	10^{-6}–10^{-7}	10^{-6}–10^{-7}	10^{-6}–10^{-7}
Triaxial	Cohesion (kPa)	5–30	10–50	30–70
Triaxial	Angle of shearing (º)	32–37	35–38	35–40
SPT	N_{SPT}, blows	10–30	30–60	>60
DPSH	Dynamic point resistance, q_d (MPa)	5–10	10–20	>20
CPTu	Cone tip resistance, q_c (MPa)	5–15	15–25	>25
CPTu	Cone side friction, f_s (kPa)	0.1–0.3	0.2–0.5	–
DMT	Material Index, I_D	1.0–3.0	1.0–3.5	1.5–3.5
DMT	Horizontal stress index, K_D	5–25	10–40	>40
DMT	Dilatometer modulus, E_D (MPa)	25–75	60–120	>100
PMT	Yield pressure, P_y (MPa)	0.5–1.5	1.0–3.0	1.0–6.0
PMT	Limit pressure, P_l (MPa)	1–3	1.5–4	2.5–10
PMT	Pressuremeter modulus, E_{PMT} (MPa)	10–25	15–40	50–150
Seismic	Primary wave, v_p (m/s)	400–800	800–1500	1250–2000
Seismic	Shear wave, v_s (m/s)	175–300	300–400	400–500

Therefore, the geotechnical ranges of both residual masses are easily and sustainably integrated, contributing to a much more robust analysis of these granitic environments and allowing for a comparison of the findings in the experimental site with the research work developed in FEUP and with the information available in the Porto Geotechnical Map [7,12].

3. Materials and methods

The initial research frame developed in the IPG experimental site aimed to deeply characterize the local granitic spot within the IPG facilities. Simultaneously, a research frame was launched by LGMC of CICCOPN dedicated to the first attempt to settle a methodology for interpreting DMT test results in granitic residual soils [1,13]. Overall, 20 pairs of CPTu-DMT tests were followed by boreholes where Shelby intact samples were retrieved for laboratory testing (oedometric, shear box, and triaxial tests). The results revealed the expected similarity of Porto and Guarda granites, allowing for the integration of characterization data from both formations. In the sequence, the first correlations to obtain strength parameters from DMT tests (cohesive intercept and angles of shearing resistance) were established by comparing test data with triaxial results. However, due to the disturbance in cementation structure arising from the sampling processes, the results of triaxial tests deviate from field reality, and so the reference for correlations reflects only partial cohesive strength.

To overcome these difficulties, a new research frame was established considering a calibration under controlled conditions (CCC), working with artificially cemented mixtures for DMT and triaxial testing, thus avoiding sampling in the process. CCC is a container (large box) with a 1.5 m height steel box, a square cross section of 1.0 m^2, and 3 mm thick steel walls reinforced by metal bars placed at one-third and two-thirds of its height. Each panel was fixed to the adjacent one with a profile of 5 screws (10 mm) with 150 mm of influence radius. Due to the panel-to-panel fixation system, in two of the faces, this reinforcement system was in contact with the wall by a central 7 mm thick H beam (100 × 50 mm) placed vertically. This system aimed to reduce horizontal displacements during compaction processes. The inner surfaces (vertical walls) and bottom surface of the cell were covered with a plastic film, in contact with the steel wall, followed by 15 mm Styrofoam plates to create a smooth and flexible transition between the soil and the external border.

Five block samples with 1 × 1 × 1.25 m^3 were created in CCC, departing from residual soils collected in a natural slope within the IPG site, one de-structured and four artificially cemented. Artificially cemented mixtures were remolded from de-structured granitic samples, adding different percentages of Portland cements to recreate different cementation magnitudes within the intervals observed in the local natural soils. Total grain size was preserved to represent the natural soil, and the same in situ conditions were reproduced, namely: unit weight (18.4 kN/m^3), moisture content (13.5%), and void ratio (0.60). The CCC specimens were obtained by dynamic compaction of the artificial mixture, prepared in layers 70–80 mm thick to obtain void ratios of the same order of the in situ magnitude of local granites, for further comparisons. The compaction in the chamber was handmade, using a round wood hammer with 40 cm diameter. Close control of the layers during compaction ensured a homogeneous block sample. In parallel, samples for triaxial testing were remolded with the same void ratios, percentages of cement, and curing times to create comparable situations. The control of strength levels was established by comparing uniaxial and diametral compressive tests performed in the natural soils and artificial mixtures. Tests were performed considering low (25, 50, and 75 kPa) and medium (300 kPa) confining stresses.

Cemented specimens prepared in the CCC chamber and triaxial testing used two types of cement. The first one was the CIM I/52.5R, which is indicated for concrete strength classes C40/50 to C50/60. This is a grey cement of high performance, usually used in the composition of rapid curing concrete when short curing times are needed to achieve final strength, with high hydration temperatures. With

this cement type, two block samples were generated with 1% and 2% of cement, with 14 days of curing. The second one was the CIM II/B-L 32.5N, which is indicated to concrete strength classes C12/15 to C25/30 and is a product of low initial strength evolution and high workability with small rates of water/cement. With this cement, two block samples were generated with 2% and 3% of cement, with 21 days of curing. These percentages and curing times were chosen to be comparable with the strength observed in natural soils. As referred above, the indexation was based on uniaxial compressive and tensile test results, instead of the cement percentage.

During the compaction, two DMT blades were installed, one 20 cm above the base level and another placed 25 cm below the surface in the upper level of the CCC specimen. Block samples were only partially saturated to allow studying the influence of suction on test results. To control the water level, two open-tube (polyvinyl chloride) piezometers were installed: one located in one corner from which the water was introduced at the base of the chamber, and the second located in the opposite corner to confirm the water arrival and the respective level stabilization. Above water level, suction measurements were obtained by means of six installed tensiometers. Finally, three pairs of geophones for seismic survey were placed along one profile to measure compression and shear wave velocities. Figure 2 shows the instrumentation within the CCC specimen, while Figure 3 provides a general view of the chamber before and after the test, during the dismantling operations. Detailed information can be found in [1]. As for triaxial testing, applied stresses were measured by submerged cells of 10 kN capacity; axial strains were obtained by internal LVDT devices, and tests were performed in consolidated drained conditions [1,14].

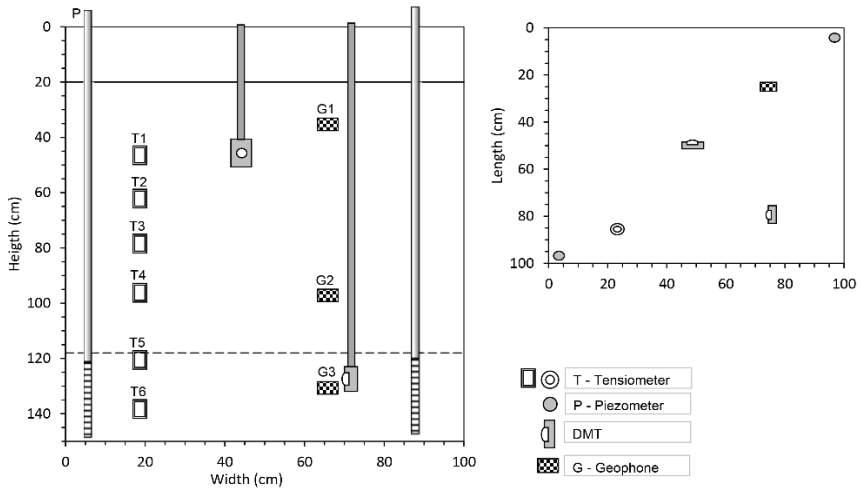

Figure 2. Plant and cross section of CCC instrumentation.

Figure 3. CCC sample before (left) and after (right) testing.

The described research frame led to the definition of proper correlations between DMT and strength parameters, according to Mohr–Coulomb failure envelopes. Furthermore, these correlations allowed the use of DMTs as a reference to obtain correlations with other in situ tests, such as CPTu and PMT. A new experimental field program was then settled in the IPG experimental site, consisting of the parallel execution of six sets of SDMT (seismic dilatometer), SCPTu (seismic piezocone), and PMT (Menard pressuremeter) tests, followed by boreholes from where intact samples for laboratory tests were retrieved (Figure 4). Tests were performed within the upper 6 m of the natural granitic spot of the IPG experimental site.

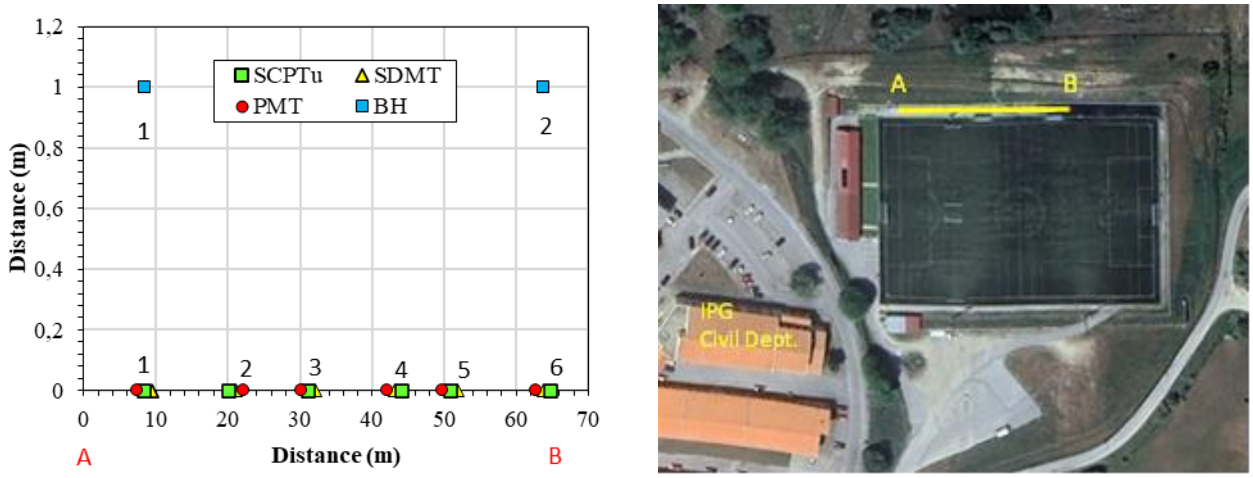

Figure 4. Testing program layout.

In this new research frame, besides strength correlations, degradation deformability modulus curves were also determined, for which the shear wave velocities obtained in SDMT and SCPTu were fundamental [2,3]. Overall, since the beginning of the research, more than 150 tests have been performed, excluding those arising from the Porto Geotechnical map, as represented in Table 2.

Table 2. Performed tests.

Phase	Performed tests
1a. Guarda residual soil	TRX (53), UCS (12), PMT (5), CPTu (8), DMT (3), CH (1)
1b. Porto residual soil	TRX (5), CPTu (20), DMT (20)
2. DMT calibration	TRX (5), UCS (30), DMT CemSoil (5), DMT (2)
3. CPTu/PMT calibrations	TRX (6), SDMT (6), PMT (18), SCPTu (6)

The seismic dilatometer (SDMT) and seismic piezocone (SCPTu) used in the experimental work are the combination of the respective mechanical tests, respectively standardized in ASTM D6635-15 [15] and ASTM D5778-20 [16], with a seismic module for measuring the shear wave velocity (V_s) that follows ASTM D7400-19 Standard Test Methods for Downhole Seismic Testing [17]. PMT tests followed ASTM D4719/ [18] and triaxial testing ASTM D-7181 [19].

4. Results and discussion

4.1. Laboratory testing in unstructured, natural, and artificially structured samples

An extensive set of uniaxial and diametral compression tests was first carried out on natural and artificially cemented samples, aiming to define which cement composition (type and percentage) generated the same value of diametral compression resistance, which is directly related to the cohesive portion of the shear resistance. A summary of the results obtained is shown in Figure 5, where it becomes obvious that the composition and behavior of natural soils fall between the compositions of 1% cement CIM52R and 2% cement CIM32.5N.

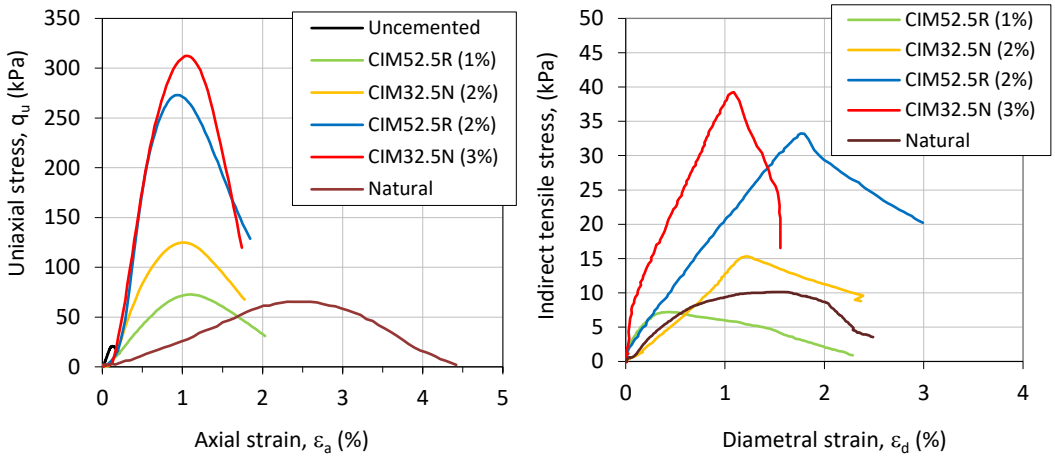

Figure 5. Uniaxial compression and indirect tensile tests in natural and artificially cemented soils.

In order to understand the effect of the structure on the shear strength and stress-strain behavior, a vast program of triaxial tests with different stress paths was carried out on structured and unstructured natural samples (molded with similar void ratios). Figure 6 illustrates the different behavior revealed by these samples in CID triaxial tests, clearly revealing that, unlike natural samples, there is no clear peak of deviatoric stress in the unstructured samples, and natural structured samples reveal stronger

dilatancy. Furthermore, the same figure also shows that the peak resistance of structured samples is mobilized at higher levels of strain for similar confining stresses.

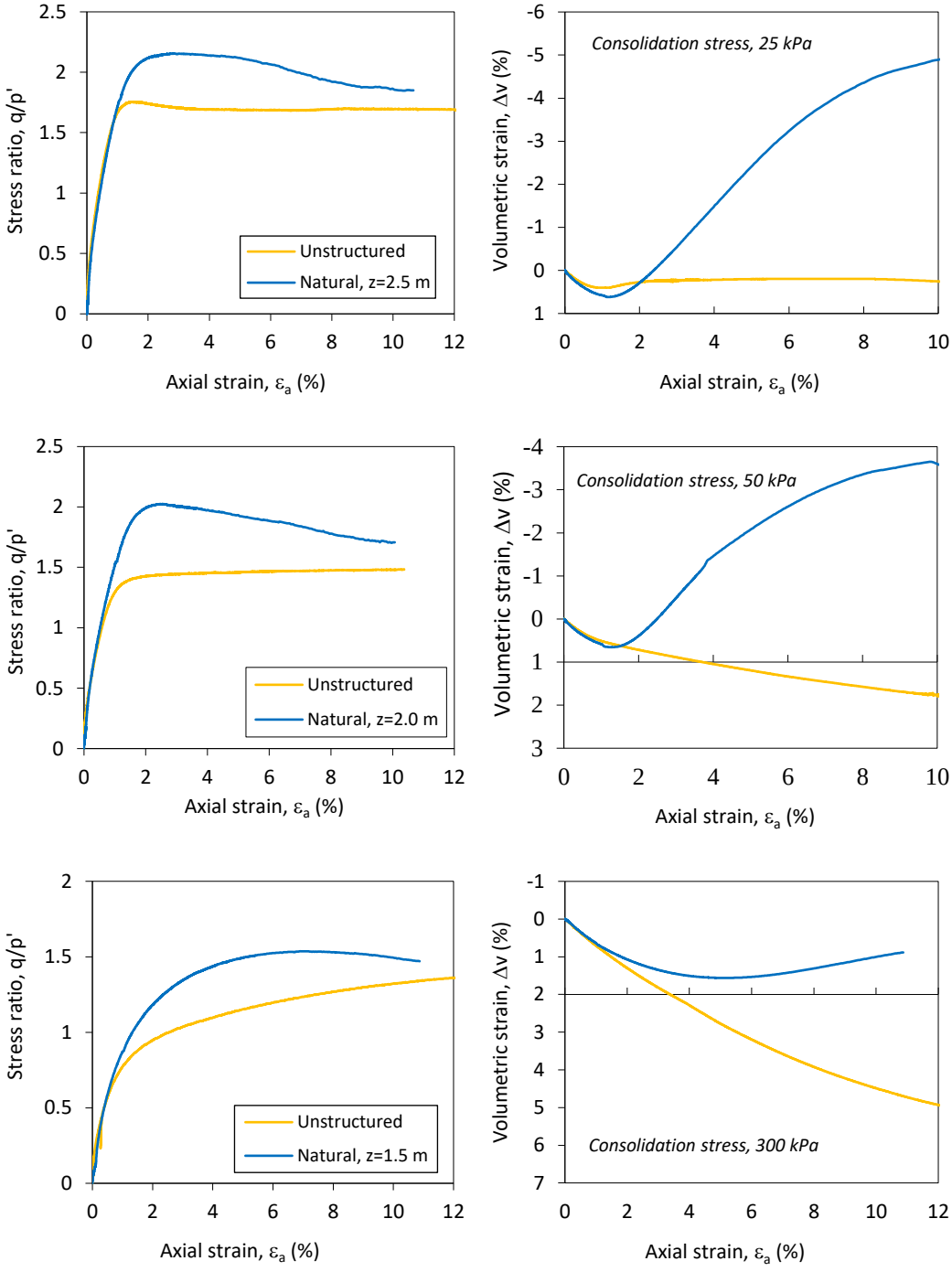

Figure 6. CID triaxial results at low and medium confining stresses in structured and unstructured natural samples.

The main results obtained in triaxial testing performed in artificially cemented mixtures within the main DMT calibration experiment are summarized in Figures 7 and 8.

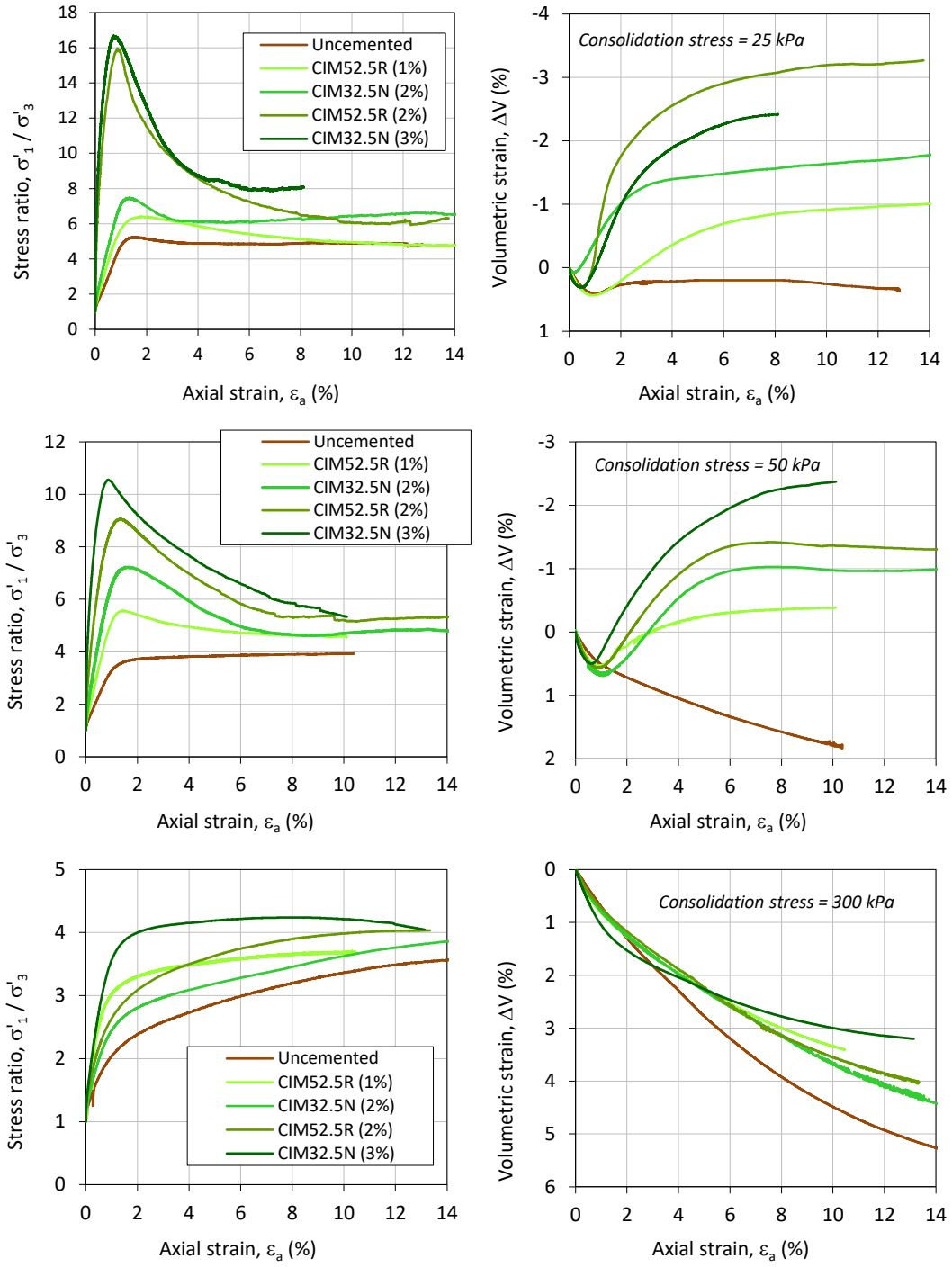

Figure 7. CID triaxial results at low and medium confining stresses in artificial samples.

The main considerations arising from these results can be summarized as follows:

a) Unstructured samples show ductile behavior, apart from a smooth peak at lower confining stress (25 kPa), explained by the approach of uniaxial conditions.

b) Artificial mixtures reveal the development of an increasing peak strength with cementation level, which, in turn, is limited by a certain level of initial mean effective stress, after which frictional strength takes control.

c) At low confining stresses (25–75 kPa), stress-strain curves reveal brittle failure modes,

followed by dilatant behavior, with increasing values with cementation level, while peak axial strains decrease with cement content, ranging between 2% and 0.8%. At high confining stresses (300 kPa), stress-strain curves reveal ductile contractive behavior with maximum strength obtained for higher strains (8% to 18%).

d) Stress-strain curves also reveal an increasing initial stiffness with cementation level, while dilatant behavior increases with cementation level and decreases with initial mean effective stress.

e) The representation of failure envelope in p'-q space (Figure 8) reveals a linear development for unstructured samples, while artificial mixtures show nonlinearity, more pronounced as cementation level increases.

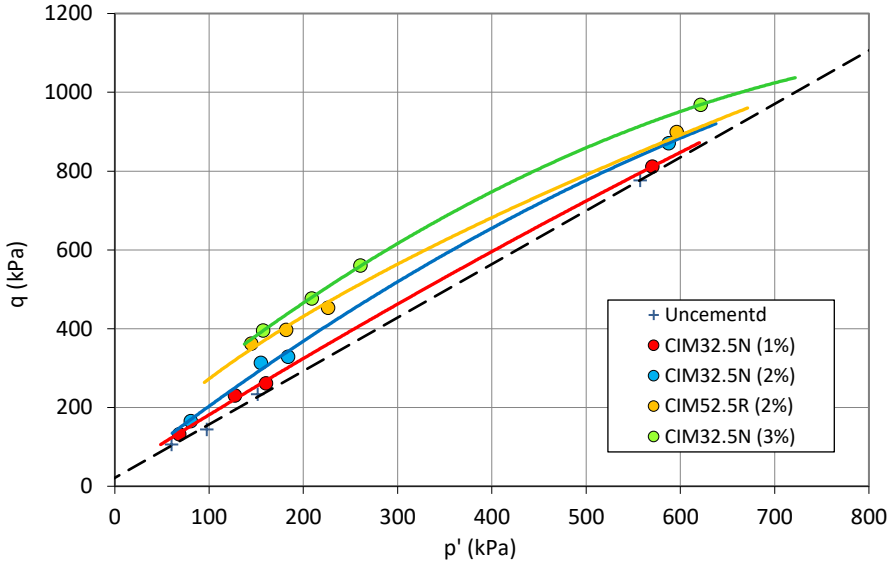

Figure 8. Strength envelopes in q-p' stress space (artificial samples).

Finally, Figure 9 compares the stress-strain behavior of the structured and unstructured natural soil samples with the artificially cemented soil samples in CID triaxial tests. As can be observed, artificial mixtures and natural soil generate similar strength behavior and magnitude, while the stress-strain behavior can be quite different. In fact, the natural soil reveals that peak resistance occurs at higher strain levels than those observed in artificial mixtures. Furthermore, the natural soil also shows higher dilatancy when compared with artificial mixtures, revealing that the natural soil fabric, inherited and preserved from the original rock massif, has a major influence on the strain behavior of these granitic residual soils.

4.2. (S)DMT and (S)CPTu tests

Seismic dilatometer and piezocone tests are highly interchangeable; thus, the investigation presented herein was greatly based on pairs of these tests, since the beginning of the program. Obtained results in the granitic residual masses show that CPTu and DMT sedimentary-based methodologies [20,21] correctly identify the presence of silty sand to sandy silt soils, sustainably

validated by the laboratory identification tests. Similar conclusions can be obtained from the unit weight determinations based on sedimentary approaches [20], revealing convergence between the results obtained in both tests with the laboratory evaluations performed in intact Shelby samples (Figure 10). This is particularly important since some intermediate DMT and CPTu test parameters used in the correlations with geotechnical parameters depend on the in situ stresses.

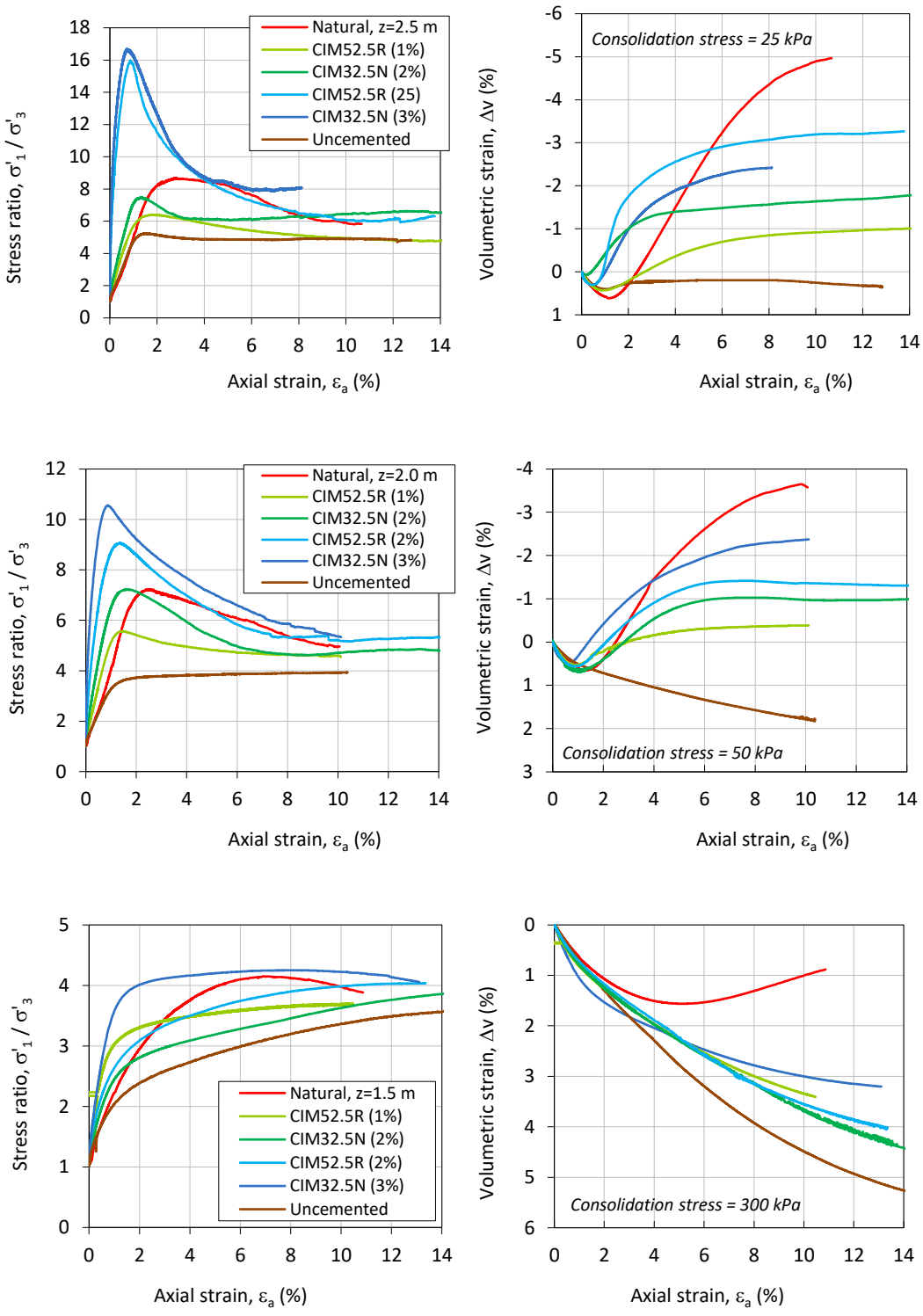

Figure 9. CID triaxial results at low and medium confining stresses in natural and artificial samples.

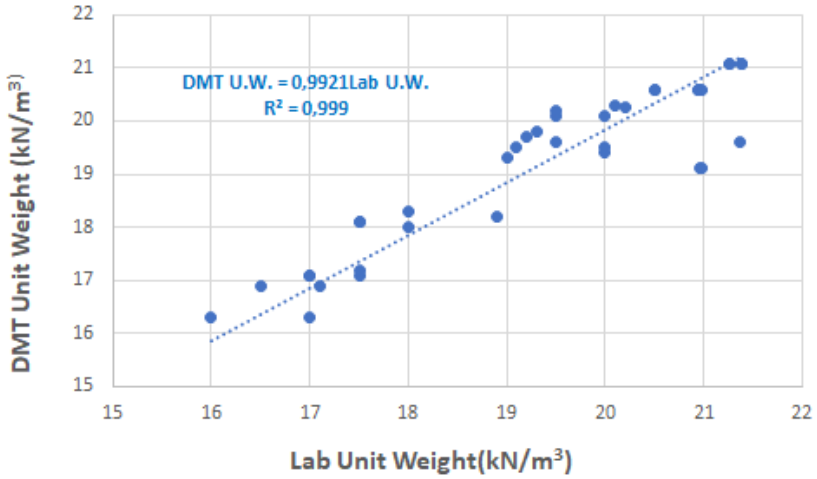

Figure 10. DMT vs. laboratory unit weights.

Regarding the drainage conditions observed during test execution, once again, CPTu and DMT results are convergent and supported by the characteristics observed in the laboratory tests. Figure 11 represents the obtained pore pressure indexes, U_D (pore pressure index) and B_q (normalized pore pressure ratio), related to DMT [20] and CPTu tests [21], respectively. U_D and B_q equal to "0" means that a drained condition is attained, while increasing values of both parameters reflect a drop in draining ability. U_D and B_q are defined by Equations 1–5:

$$U_D = \frac{P_2 - u_0}{P_0 - u_0} \tag{1}$$

$$P_0 = 1.05(A - Zm - \Delta A) - 0.05(B - Zm - \Delta B) \tag{2}$$

$$P_2 = C - Zm - \Delta A \tag{3}$$

where P_0 and P_2 are the corrected DMT lift-off and closing pressures, respectively, u_0 is the in situ pore pressure, ΔA and ΔB the calibration pressures of the membrane, A, B, and C are the field DMT test readings, and Z_m is the manometric zero.

$$B_q = \frac{u_2 - u_0}{q_t - \sigma_{v0}} \tag{4}$$

$$q_t = q_c(1 - a) \tag{5}$$

where u_2 and u_0 are the pore pressure at tip level and in situ pore pressure, respectively, σ_{v0} is the in situ vertical stress, q_c is the net cone resistance, and "a" is the cone parameter.

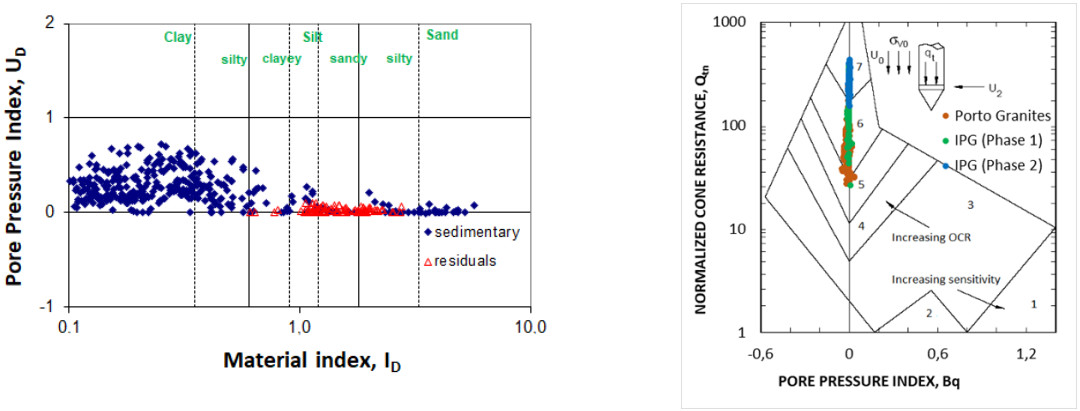

a) b)

Figure 11. Pore pressure indexes: a) DMT [20]; b) CPTu [21].

Furthermore, the soil behavior type (SBT) obtained from both tests [22,23] confirms the previous considerations and converges toward the same dilative behavior in shear (Figures 12) that was observed in previously presented triaxial tests performed at equivalent (low) confining stresses.

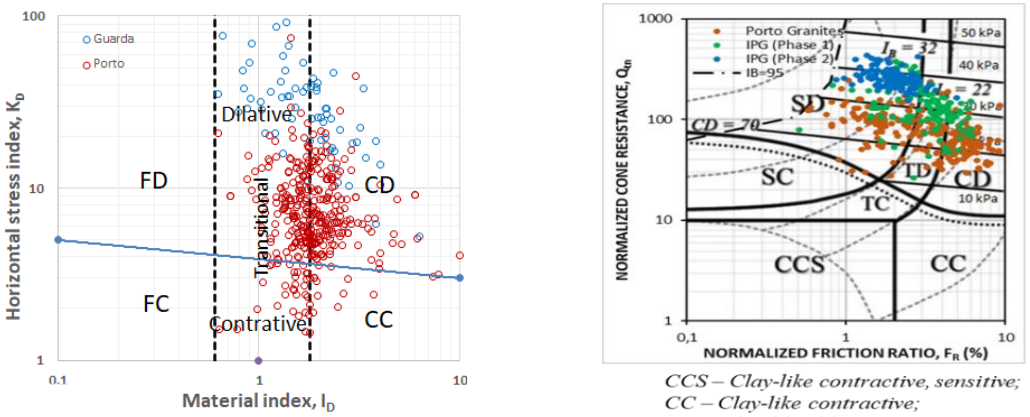

CD – Coarse grained dilative (mostly drained)
CC – Coarse grained contractive (mostly drained)
FD – Fine grained dilative (mostly undrained)
FC – Fine grained dilative (mostly undrained)

CCS – Clay-like contractive, sensitive;
CC – Clay-like contractive;
CD – Clay-like dilative;
TC – Transitional contractive;
TD – Transitional dilative;
SC – Sand-like contractive;
SD – Sand-like dilative

a) b)

Figure 12. SBT diagrams: a) DMT [22]; b) CPTu [23].

Once residual and sedimentary soils are represented by different behaviors related to the presence or absence of cementation, it becomes fundamental to discern them in order to decide the best set of correlations to be used in each parametrization. Figure 13, proposed by Cruz et al [24] and Robertson [23], sustainably detects the cementation of Portuguese saprolites and can be quite useful for that purpose.

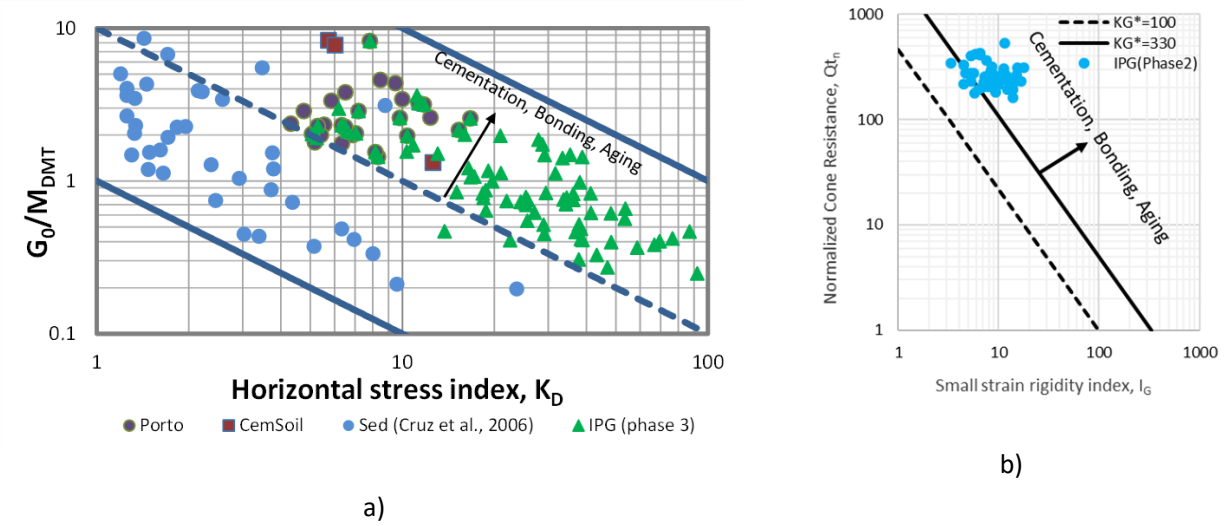

Figure 13. Identifying cemented structure: a) DMT [24]; b) CPTu [23].

Portuguese granitic residual soils are cohesive-frictional materials, thus represented by a cohesive intercept and an angle of shearing resistance, while sedimentary approaches only allow for the determination of one single parameter for each drainage condition. Therefore, cohesion intercept cannot be evaluated, and the angle of shearing resistance is systematically overpredicted by incorporating the cohesive contribution. The approach to solve this problem was based on the similar behavior observed in residual soils and sedimentary clays, consisting of a sharp break in stress-strain curves that is related to the breakage of cementation structure in residual soils and attaining the pre-consolidation pressure in sedimentary soils [1,13]. As a consequence, test parameters related to pre-consolidation pressure and/or overconsolidation ratios were selected to calibrate a DMT correlation with a cohesive intercept. The best result was obtained by using the Marchetti and Crapps sedimentary OCR correlation [25], and the parameter was renamed virtual OCR, since the true concept of OCR is not applicable to residual soils [1]. Figure 14 shows the correlation between global cohesion (integrates cohesion and suction, when the latter is present) and virtual OCR, obtained in the CCC tests [1]. The goodness of fit may be accessed via the coefficients of determination ($R^2 = 0.836$), also presented in Figure 14. These promising results support the relevance of this initial approach and justify its extension to larger datasets for broader validation and refinement. Moreover, the regression analysis demonstrates a statistically significant model, that besides the previously referred coefficient of determination (R^2) around 0.836, is supported by an F-statistic of 29.07 and a corresponding p-value of 0.0017 (<<0.01), indicating the model's robustness and the relevance of the predictor variable in explaining the observed data. In the same figure, the correlation deduced by Cruz et al. in 2006 [13] based on triaxial testing is also presented. Note that the differences between the two correlations can be explained, at least partially, by the sampling disturbance, which affects only the earlier correlation.

Once the cohesion intercept is obtained, the overestimation of the angle of shearing resistance deduced from a sedimentary approach can be corrected, since the difference between overestimated and true angles are related with the cohesive intercept. The obtained correlations are represented by the following equations:

$$c'_g(kPa) = 7.716 \ln(vOCR) + 2.94 \quad (6)$$

$$\emptyset_{corr} = \emptyset_{sed} - 3.45\, ln(vOCR) + 8.20 \quad (7)$$

where c'$_g$ represents the cohesive intercept resulting from cementation and suction (when the latter is present), vOCR is the virtual OCR obtained by Marchetti and Crapps correlation [25], ϕ_{corr} is the corrected angle of shearing resistance, and ϕ_{sed} is the angle of shearing resistance deduced according to sedimentary approach [20].

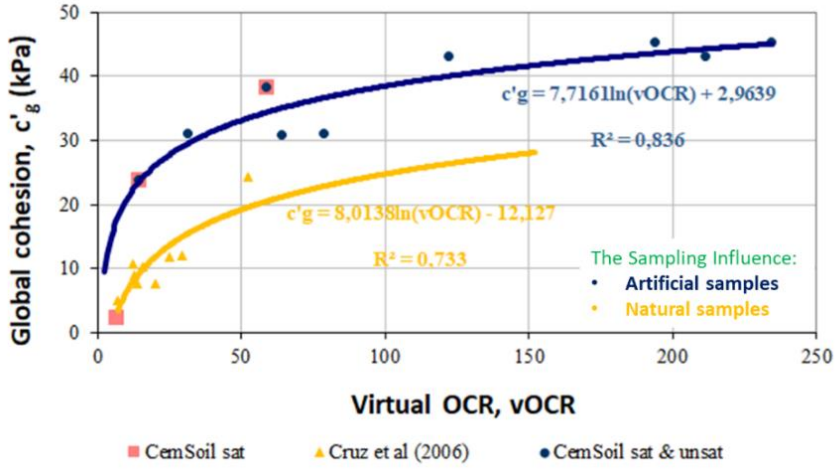

Figure 14. Correlations between virtual OCR and global cohesion.

The correlations obtained in the CCC experiment were then compared with the in situ test results of the experimental site, and later with the available data of Porto granites (FEUP and Porto Geotechnical Map), validating its application in these two formations.

Due to the well-known interchangeability between DMT and CPTu tests, the correlations dedicated to CPTu tests were obtained with the DMT results as reference [26], avoiding the complex work with the CCC apparatus. To analyze the response strength, all available data were gathered and analyzed in the Laboratory of Mathematical Engineering of the Polytechnic Institute of Porto. For global adjustments, Porto granites were used as training subsets, while IPG was selected as a testing subset, due to its connection with the DMT calibration and also because the respective data covers the whole range of measurements. The correlations obtained by this comparison with DMT-derived data can be written as follows:

$$c'_g(kPa) = \ 11.5\, ln(\, Q_{t1}) + 3.2\, ln(\, F_R) - 30.8 \quad (8)$$

$$\varphi_{corr} = \varphi_{sed} - 5.27\, ln(\, Q_{t1}) - 0.99\, ln(\, F_R) + 22.46 \quad (9)$$

where c'$_g$ represents the cohesive intercept resulting from cementation and suction (when the latter is present), while Q_{t1}, Q_{tn}, and F_R are CPTu normalized parameters.

After the calibration work, correlations were applied to all the available Porto and Guarda DMT and CPTu data, allowing the development of the isolines of cohesive magnitude represented in the SBT diagrams of Figure 15.

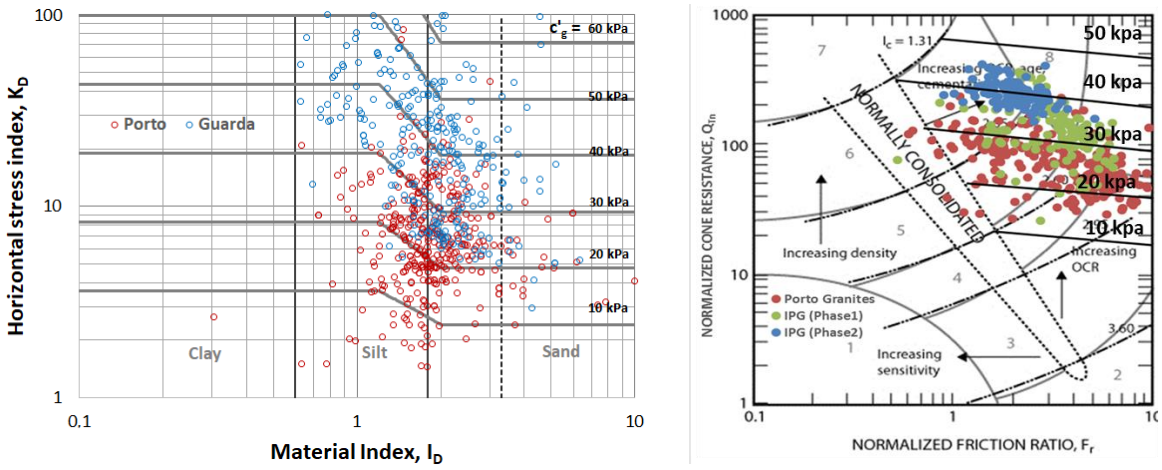

Figure 15. SBT diagrams related with cohesive intercept: a) DMT; b) CPTu.

Accordingly, deriving the strength parameters from DMT and CPTu tests in common situations should go through the following steps: 1) Evaluate whether or not the cementation structure is present (Figure 13); if shear wave velocities are not available, the presence of cementation can be detected by visual inspection or using shear tests. 2) Calculate global cohesion from equations 6 and 8, based on DMT and CPTu test parameters, respectively; above water level, global cohesion integrates both cohesion from cementation and suction, while below that level, global cohesion only reflects cementation. 3) Calculate angles of shear resistance from equations 7 and 9, based on DMT and CPTu test parameters, respectively.

From the deformability point of view, DMT is a very efficient test in modulus determinations due to its stress-strain-based evaluation, while CPTu is typically a strength test, thus less applicable for this purpose. DMT evaluations are sustained by the theory of elasticity [20] with the dilatometric modulus, E_D, deduced considering a semi-spherical expansion and adjusted as a function of the type of soil (I_D) and the level of cementation structure (K_D) to obtain the constrained modulus (M_{DMT}).

As previously stated, the typical stress-strain curves of structured soils are characterized by two yield points, one related to the beginning of yield weak bonds (1st yield) and the other one related to the complete breakage of the bond structure (bond yield or 2nd yield). The representation of SDMT test results in modulus decay curves obtained from triaxial data (Figure 16) shows that G_{DMT} results are within the same locus of the 1st yield, suggesting that equipment installation does not deeply affect the cementation structure in the measurement area. On the other hand, the maximum stiffness obtained at small strain in triaxial tests is in the same order of magnitude as that obtained by shear wave velocities, revealing the good quality achieved in sampling processes. It is also clear that the increase in cementation is followed by the increase of the working strain modulus (G_{DMT}) and the decrease of the strain level (γ_{DMT}), suggesting that the lower the level of cementation, the lower the field of the load transfer during the membrane expansion will be, which have important consequences in design.

In turn, γ_{DMT} in the natural residual soils fell within 0.002% and 0.009%, which is one order of magnitude lower than that obtained in sedimentary soils with similar grain size ($\gamma_{DMT} \approx 0.01\%–0.30\%$). This illustrates the differences in the stiffness of both soils. In artificial samples, the "working strain modulus" (G_{DMT}) is lower than that observed in natural samples, corresponding to higher γ_{DMT} and

falling in the same locus of sedimentary sandy soils found by Amoroso et al. [27]. Figure 17 represents G/G_0 vs. γ_{DMT} obtained in the triaxial tests performed in IPG, plotted together with the sedimentary results presented by Amoroso et al. [27].

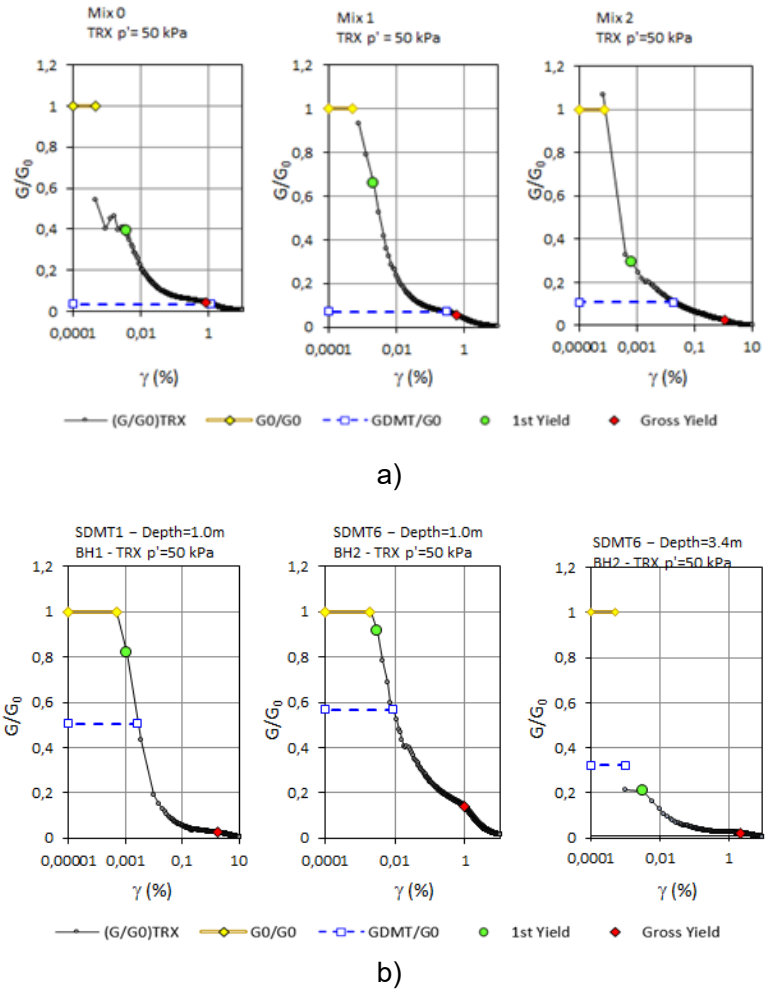

Figure 16. Modulus decay in: a) artificial soils; b) natural soils.

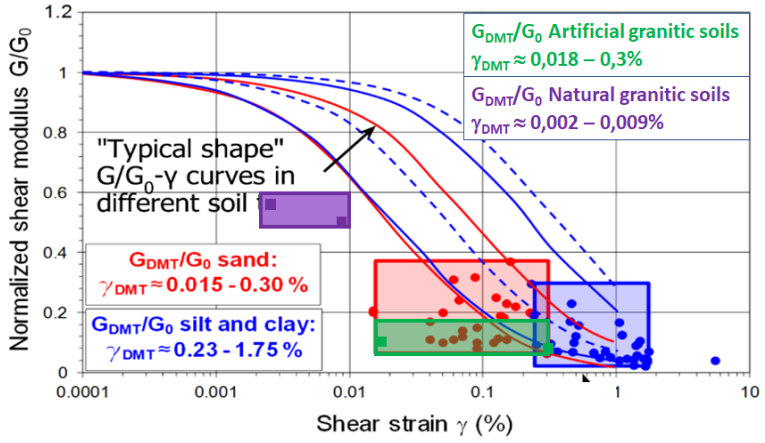

Figure 17. Representation of residual soil G_{DMT}/G_0 together with sedimentary soils (adapted from Amoroso et al. [27]).

The observed differences confirm the perceived influence of the fabric in the overall stress-strain response and reveal the difficulty of artificial samples to represent natural soils in terms of deformability. A detailed discussion of this subject can be found in [1].

The appropriate modulus to be used in a specific context is much improved if the modulus decay curve is settled, which is much more difficult to obtain in situ than in laboratory tests. In SDMT tests, two different deformability moduli corresponding to different strain levels are obtained; one corresponding to very small strains obtained from shear wave velocities, and another corresponding to working strains obtained by the mechanical response of the test. This opens a window of opportunity to establish the moduli decay curve. Following the general agreement of using a hyperbolic stress-strain relationship to represent the behavior of soil within small-to-medium strain levels, Amoroso et al. [27] proposed a specific model to be used in the case of SDMT sedimentary data, represented by the equation (10):

$$\frac{G}{G_0} = \frac{1}{1 + \left(\frac{G_0}{G_{DMT}} - 1\right)\frac{\gamma}{\gamma_{DMT}}} \tag{10}$$

where G_0 and G_{DMT} are the maximum and DMT shear modulus, G is the shear modulus, γ is the shear strain, and γ_{DMT} is the DMT shear strain.

The application of this model to the data obtained in the IPG experimental site revealed poor convergence, deviating considerably at medium and high strain, underestimating the stiffness of the natural soil. Therefore, other mathematic formulations based on SDMT data were studied, leading to the development of the logistic curve expressed below [28]:

$$G = \frac{a}{(1 + e^{-b(log(\gamma) - c)})} \tag{11}$$

where $\lim_{\gamma \to 0} G(\gamma)$ is the logistic horizontal asymptote, b (<0) is the gradient of the curve, and c is the natural logarithm transformed x-value of the curve's midpoint.

Departing from this logistic curve, an attempt was made to correlate a, b, and c, which define the equation, with the DMT test parameters. Concerning "a", since b < 0, and $\lim_{\gamma \to 0} \frac{G}{G_0} = 1$, it is straightforward that the parameter should be equal to G_0. Note that by taking a = G_0, b = −1, and $c = -log\left(\frac{G_0 - G_{DMT}}{G_{DMT} \times \gamma_{DMT}}\right)$, Equation (10) is obtained.

To obtain "b" and "c", various DMT parameters were considered, searching for the most relevant fit. For each dataset resulting from the described experiences, the logistical model was adjusted regarding its parameters, a (=G_0), b, and c, and using weighted least squares, since the datasets were not uniformly distributed along all the gamma values. Thereafter, each (a, b, c) triplet that provided the best fit to the respective data set was combined with all the SDMT parameters, and several combinations/functions of those parameters were tested, using MATLAB R2016b. The best fits showed that the parameter b is better correlated with vOCR, and parameter c correlated with a combination of G_0 (MPa) and K_D, as represented below:

$$b = 0.0004406vOCR - 0.5591 \tag{12}$$

$$c = -4.041 - 0.02774G_0 + 0.03388K_D \tag{13}$$

The application of the model produced a reasonable overlap with the decay curves obtained from triaxial testing in natural and artificial samples [28]. This means that despite the differences observed in the strain level and modulus degradation of the two types of samples, the model can properly represent both (Figure 18).

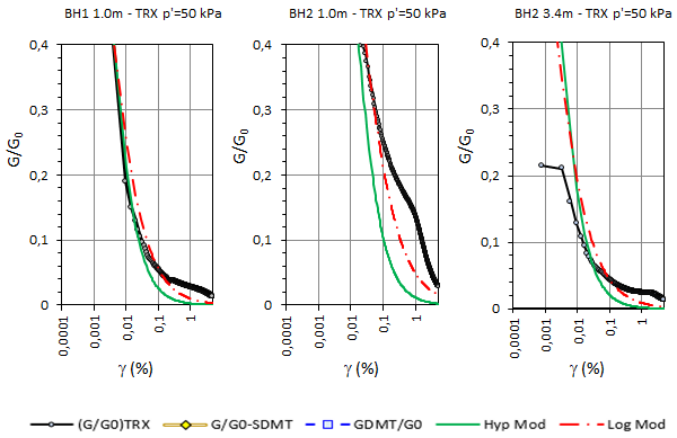

a)

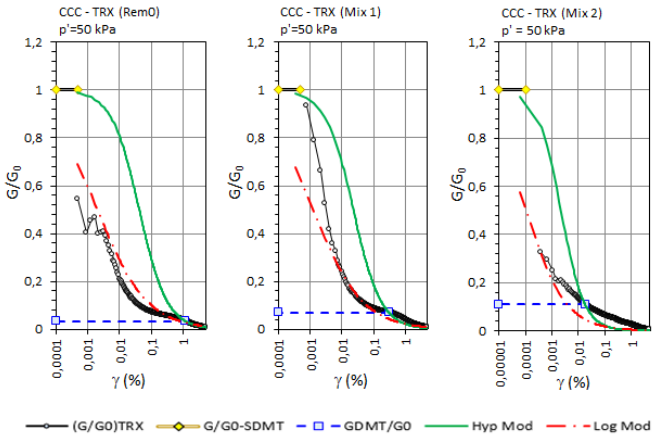

b)

Figure 18. Modulus decay deduced from hyperbolic and logistic models: a) natural soils; b) artificial soils.

The proposed methodology relied on the availability of data sets from different locations, each with several observations to fit the best parametrization for each site. However, those paired datasets are not easily available since they need both DMT and shear wave velocities test results performed in the same location, as well as triaxial testing for comparison purposes. As a consequence, there was not enough data to perform a cross-validation methodology, which is the aim of future work. In this sense,

the presentation of this methodology herein may allow other researchers to share new datasets in order to achieve and assess the robustness of the model.

4.3. PMT tests

The available PMT data is scarce and only available in the IPG experimental site; thus, a different approach had to be followed [29]. In this case, the angle of shearing resistance was first evaluated following the proposals of Menard [30] and Hughes et al. [31]. The obtained ranges led to completely different results, [34º to 36º] and [46º to 53º], respectively, with the former converging to corrected results obtained via DMT and/or CPTu. These differences found a reasonable explanation in the strain levels related to each correlation. In fact, the Menard proposal is based on limit pressure, while the proposal by Hughes et al. is placed within the pseudo-elastic phase (that is, between lift-off and yield pressures), generating results related to different strength stages. The former corresponds to a stage level near failure when cementation structure is not present anymore, while the latter corresponds to a strength stage where the cementation is still present. As a consequence, the proposal by Menard will correspond to the real angle of shearing, while that of Hughes et al. integrates friction and the still available cementation resistance; the difference between results is related to the cementation strength. As such, considering the result obtained by Menard's as the true angle of shearing, it is possible to deduce the cohesive intercept using the Mohr–Coulomb failure envelope, as represented in Figure 19 and described below:

1) Represent in the Mohr–Coulomb stress space (τ-σ_N) the envelopes of both proposals, starting from the origin (envelopes labeled with 1 and 2 in the figure).
2) Define the in situ effective stress corresponding to the PMT depth of execution and draw a vertical line up to envelope 2 (label 3 in the figure).
3) Draw a line parallel to envelope 1 passing through the intersection defined in 3 (label 4 in the figure).
4) Calculate the intersection of line 4 with the shear stress axis, which corresponds to the cohesive intercept.

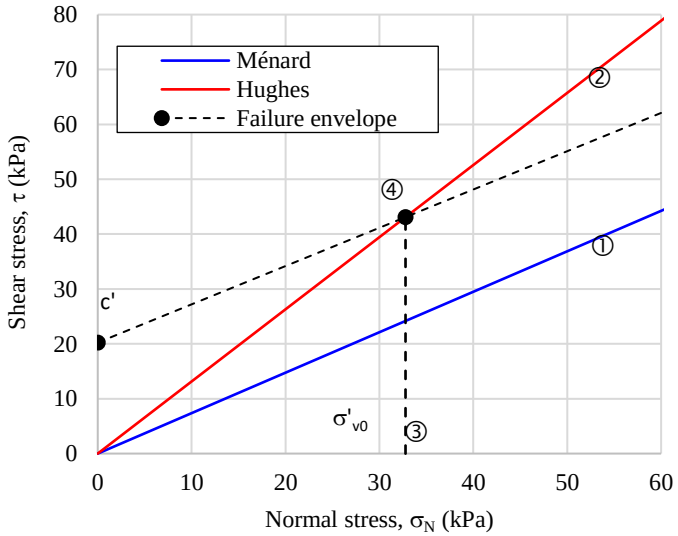

Figure 19. Estimation of shear strength parameters from PMT tests in residual soils.

Figure 20 represents the parametric comparison between PMT and DMT/CPTu results, revealing a fair convergence.

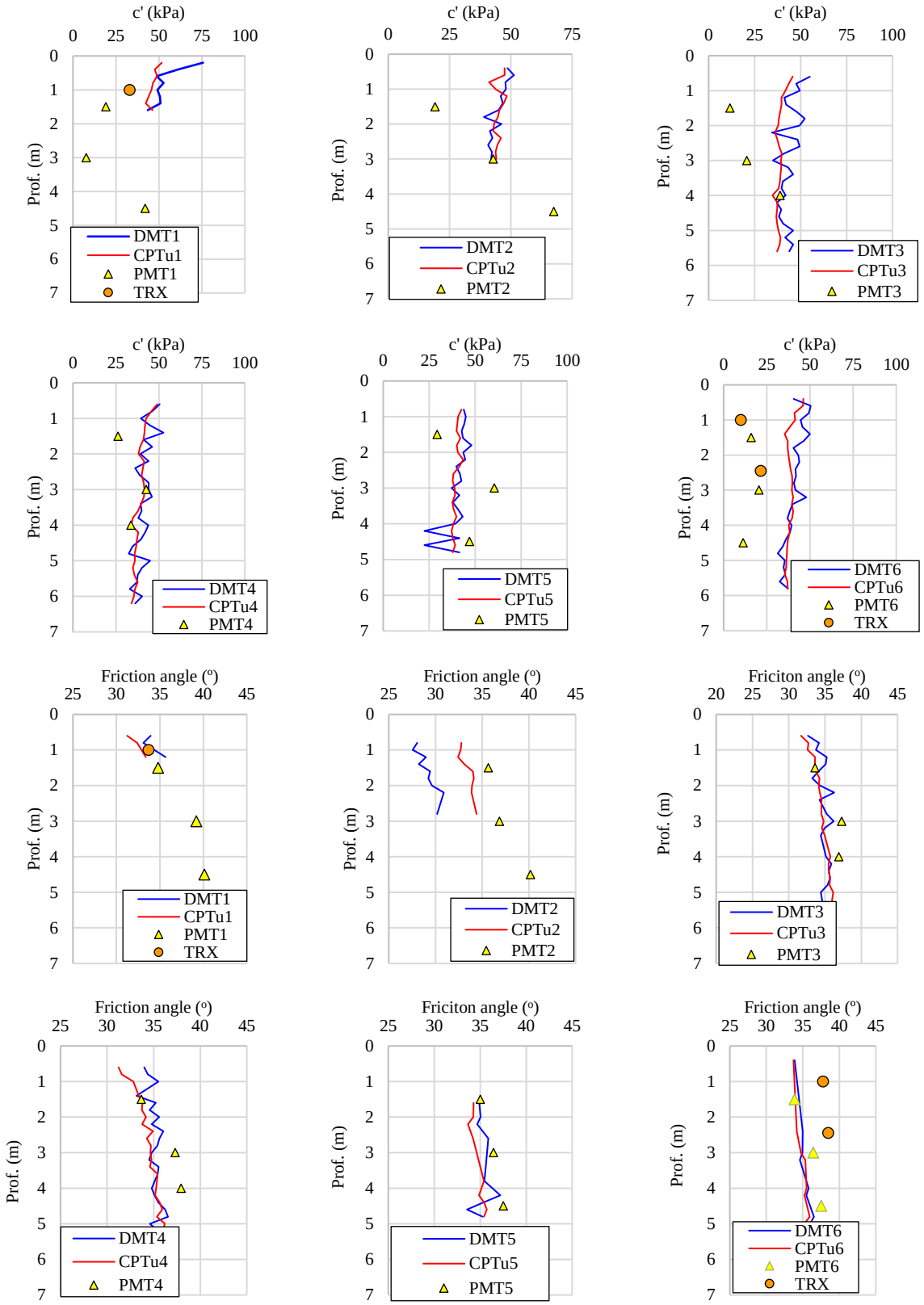

Figure 20. Shear strength parameters obtained by different tests, PMT, CPTu, and DMT, conducted at six different points.

5. Conclusions

The work performed since 2003 in the IPG experimental site has allowed for the development of specific correlations and methodologies applicable to the residual masses of Porto and Guarda granites. The work conducted can be summarized as follows:

a) The obtained information in Porto and Guarda granitic formations is very extensive and varied, incorporating laboratory and in situ tests; laboratory tests include triaxial, shear box, and triaxial tests performed on natural and artificial samples, while in situ tests include dynamic (SPT, DPSH), SDMT, SCPTu, PMT, and seismic tests; the performed study showed the behavior similarity between Porto and Guarda granitic formations, allowing for their integration.
b) Based on the data obtained in the IPG site, it was possible to settle new methodologies and correlations for adequately deriving shear strength parameters from DMT, CPTu, and PMT test results; the proposed methodologies are applicable to the studied residual soils but need further validations on other granitic environments or in residual soils of different nature.
c) DMT and CPTu tests revealed high potential in the present residual soil characterization; both tests are able to identify the type of tested soils, the presence of cementation structures, the behavior in shear, and pore-pressure conditions; furthermore, they allow to correctly evaluate unit weights, cohesive intercept, and angles of shearing resistance.
d) In the case of PMT tests, the amount of retrieved data is quite lower than that obtained in the DMT and CPTu tests, which creates more difficulties in obtaining robust correlations; however, it was possible to settle a methodology that seems reasonable for strength parameter determinations.
e) As for stiffness, only DMT data allowed for a sustainable correlation; the IPG experimental data allowed for the development of a logistic model for obtaining moduli decay curves that seems to work better than the hyperbolic model in the studied soils.

Use of AI tools declaration

The authors declare they have not used Artificial Intelligence (AI) tools in the creation of this article.

Conflict of interest

The authors declare no conflict of interest.

References

1. Cruz N (2010) Modelling geomechanics of residual soils by DMT tests. University of Porto. PhD Dissertation. Available from: http://web.archive.org/web/20190326185829/https://nbdfcruz.wordpress.com/phd/.

2. Rodrigues C, Amoroso S, Cruz N, et al. (2016) G-gamma decay curves in granitic residual soils by seismic dilatometer. *5th International Conference Geotechnical and Geophysical on Site Characterization*, Brisbane, Australia. 1137–1142.
3. Cruz N, Rodrigues C, Sousa JA, et al. (2024) Effect of soil structuring on stiffness evaluated by triaxial and seismic flat dilatometer tests. *8th Int Symposium on Deformation Characteristics of Geomaterials (ISDCG2023)*, Porto, Portugal. https://doi.org/10.1051/e3sconf/202454405008
4. Peel MC, Finlayson BL, McMahon TA (2007) Updated world map of the Köppen-Geiger climate classification. *Hydrol Earth Syst Sci* 11: 1633–1644. https://doi.org/10.5194/hess-11-1633-2007
5. Viana da Fonseca A (1996) Geomechanics of Porto residual soil from granite. Project criteria for direct foundations. PhD Dissertation, University of Porto.
6. Rodrigues CMG (2003) Caracterização geotécnica e estudo de comportamento geomecânico de um saprólito granítico da Guarda. PhD Dissertation, University of Coimbra (in Portuguese).
7. COBA, Carta Geotécnica do Porto. COBA and Faculty of Sciences of University of Porto. Porto City Hall. 2003.
8. Begonha AJ (1989) Alteração das rochas graníticas do Norte e Centro de Portugal. Uma contribuição. MSc Dissertation, Universidade Nova de Lisboa (in Portuguese).
9. ASTM D 2487–17, Standard Practice for Classification of Soils for Engineering Purposes (Unified Soil Classification System). Classification of soil for engineering purposes. American Society for Testing Materials. https://DOI.org/10.1520/D2487-17R25
10. Wesley LD (1988) Engineering classification of residual soils. *International conference on geomechanics in tropical soils* 1: 77–84.
11. Lumb P (1962) The properties of decomposed granite. *Géotechnique* 12: 226–243. https://doi.org/10.1680/geot.1962.12.3.226
12. Cruz N, Gomes C, Rodrigues C, et al. (2015) An approach for improving Wesley Engineering Classification. The case of Porto Granites. *XVI European Conference on Soil Mechanics and Geotechnical Engineering*, Edimburgh, UK. 13–17.
13. Cruz N, Viana da Fonseca A (2006) Portuguese experience in residual soil characterization by DMT tests. *2nd International Conference on the Flat Dilatometer*, Washington D.C., USA. 359–364.
14. Cruz N, Rodrigues C, Viana da Fonseca A (2014) An approach to derive strength parameters of residual soils from DMT results. *Soils Rocks* 37: 195–209.
15. ASTM D6635–01, Standard Test Method for Performing the Flat Plate Dilatometer. https://DOI.org/10.1520/D6635-01
16. ASTM D5778–20, Standard Test Method for Electronic Friction Cone and Piezocone Penetration Testing of Soils. https://DOI.org/10.1520/D5778-20
17. ASTM D7400/D7400M–19, Standard Test Methods for Downhole Seismic Testing. https://DOI.org/10.1520/D7400_D7400M-19
18. ASTM, Standard Test Method for Prebored Pressuremeter Testing in Soils, 2000. https://DOI.org/10.1520/D4719-20
19. ASTM D7181-11, Standard Test Method for Consolidated Drained Triaxial Compression Test for Soils. Available from: https://store.astm.org/d7181-20.html
20. Marchetti S (1997) The flat dilatometer design applications. *III Geotechnical Engineering Conference*, Keynote Lecture 1: 421–448.

21. Robertson PK, Cabal KL (2010) Guide to Cone Penetration Testing for Geotechnical Engineering. *6th Ed Gregg Drilling & Testing.*
22. Robertson PK (2016) Cone penetration test (CPT)-based soil behaviour type (SBT) classification system—an update. *Can Geotech J* 53: 1910–1927. https://doi.org/10.1139/cgj-2016-0044
23. Robertson PK (2015) Soil Behavior Type using the DMT. *3rd International Conference on Flat Dilatometer*, Rome, Italy.
24. Cruz N, Mateus C, Cruz J, et al. (2021) Behaviour of Portuguese granitic residual soils represented in DMT and CPTu soil behaviour type (SBT) charts. *6th International Conference on Geotechnical and Geophysical Site Characterization*, Budapest, Hungary
25. Marchetti S, Crapps DK (1981) Flat dilatometer manual, *Internal report of GPE Inc*, USA.
26. Cruz N, Cruz J, Rodrigues C, et al. (2018) Behaviour of granitic residual soils assessed by SCPTu and other in-situ tests. *4th Int Symposium on Cone Penetration Testing*, Delft, Netherlands, CRC Press. 241–247.
27. Amoroso S, Monaco P, Lehane B, et al. (2014) Examination of the potential of the seismic dilatometer (SDMT) to estimate in situ stiffness decay curves in various soil types. *Soils Rocks* 37: 177–194.
28. Rodrigues C, Cruz N, Amoroso S, Cruz M (2020) Stiffness decay in structured soils by seismic dilatometer. *Geotech Test J* 43: 1003–1021. https://doi.org/10.1520/GTJ20180352
29. Rodrigues C, Cruz N, Mateus C (2024) Deriving strength parameters of granitic residual soils from Ménard pressuremeter tests. *7th International Conference Geotechnical and Geophysical on Site Characterization*. Barcelona, Spain.
30. Ménard L (1957) Mesure in situ des propriétés physiques des sols. *Ann Ponts Chaussées* 127: 356–377.
31. Hughes JMO, Wroth CP, Windle D (1977) Pressuremeter tests in sands. *Géotechnique* 27: 455–477. https://doi.org/10.1680/geot.1977.27.4.455

AIMS Press